A statistical comparison of interplanetary shock and CME propagation models

K.-S. Cho,[1,2] Y.-J. Moon,[1,3] M. Dryer,[4,5] C. D. Fry,[5] Y.-D. Park,[1] and K.-S. Kim[2]

Received 9 May 2003; revised 19 September 2003; accepted 26 September 2003; published 20 December 2003.

[1] We have compared the prediction capability of two types of Sun-Earth connection models: (1) ensemble of physics-based shock propagation models (STOA, STOA-2, ISPM, and HAFv.2) and (2) empirical CME propagation (CME-ICME and CME-IP shock) models. For this purpose, we have selected 38 near-simultaneous pairs of coronal mass ejections (CMEs) and metric type II radio bursts. By applying the adopted models to these events, we have estimated the time difference between predicted and observed arrivals of interplanetary (IP) shocks and ICMEs at the Earth or L1. The mean absolute error of the shock arrival time (SAT) within an adopted window of ±24 hours is 9.8 hours for the ensemble of shock propagation models, 9.2 hours for the CME-IP shock model, and 11.6 hours for the CME-ICME model. It is also found that the success rate for all models is about 80% for the same window. The results imply that the adopted models are comparable in their prediction of the arrival times of IP shocks and interplanetary CMEs (ICMEs). The usefulness of these models is also discussed in terms of real-time forecasts, underlying physics, and identification of IP shocks and ICMEs at the Earth. *INDEX TERMS:* 2722 Magnetospheric Physics: Forecasting; 7519 Solar Physics, Astrophysics, and Astronomy: Flares; 7513 Solar Physics, Astrophysics, and Astronomy: Coronal mass ejections; 2139 Interplanetary Physics: Interplanetary shocks; 2111 Interplanetary Physics: Ejecta, driver gases, and magnetic clouds; *KEYWORDS:* space weather forecasting, solar flares, CMEs, interplanetary shocks

Citation: Cho, K.-S., Y.-J. Moon, M. Dryer, C. D. Fry, Y.-D. Park, and K.-S. Kim, A statistical comparison of interplanetary shock and CME propagation models, *J. Geophys. Res.*, *108*(A12), 1445, doi:10.1029/2003JA010029, 2003.

1. Introduction

[2] Most disturbances of the space environment are thought to originate from various kinds of solar transient dynamic features such as type II bursts, solar flares, and coronal mass ejections (CMEs). In this respect, prediction of their arrival times at the Earth several days in advance has been regarded as an important ingredient of space weather prediction objectives. That is, arrival of these transient disturbances implies the possible initiation of geomagnetic storms if sufficiently long and sufficiently large-magnitude southward components of the interplanetary magnetic field (IMF) follow the shock and/or are contained within the CMEs.

[3] An interplanetary (IP) shock is detected when simultaneous jumps in plasma and magnetic field properties of solar wind are observed in the reference frame of a moving spacecraft [*Kartalev et al.*, 2001]. The IP shock is a disturbance propagating into and through the expanding solar wind. If the disturbance is sufficiently energetic, a portion of the shock can arrive at Earth regardless of its source location on the Sun. In this case, fast forward (FF) shocks are most common in the solar wind. All the physical parameters such as plasma density, temperature, plasma speed (in the spacecraft frame), and magnetic field strength abruptly increase at the FF shock discontinuity in accordance with the Rankine-Hugoniot conditions.

[4] A CME that is associated with a solar flare and that travels into the IP medium with its plasma structure and some form of magnetic field pattern is called an interplanetary coronal mass ejection (ICME). According to *Gopalswamy et al.* [2001], it can be classified into two types: magnetic cloud (MC) and ejecta (EJ). The MC is an extension of magnetic flux ropes (via eruptive filaments) into IP space with a high magnetic field, smooth north-south or east-west rotation, low IMF variance, and low plasma beta [*Burlaga*, 1995]. In the case of EJ, the smooth rotation may not be present because it does not have a distinct magnetic flux rope. This latter and probably most common case is often characterized (L. Burlaga, private communication, 2002) as ''complex.'' In a recent study (Table 2 of *Cane and Richardson* [2003]), the fraction of ICMEs that have magnetic cloud structures was, on average, 25% during the 1996–2002 period. Thus identifications of ICMEs (EJs)

[1]Korea Astronomy Observatory, Daejon, Korea.
[2]Department of Astronomy and Space Science, Kyung Hee University, Kyunggi, Korea.
[3]Big Bear Solar Observatory, New Jersey Institute of Technology, Big Bear, California, USA.
[4]Space Environment Center, National Oceanic and Atmospheric Administration, Boulder, Colorado, USA.
[5]Exploration Physics International, Inc., Huntsville, Alabama, USA.

0148-0227/03/2003JA010029$09.00

are frequently ambiguous and difficult [cf. *Gopalswamy et al.*, 2001, Table 2]. The arrival of CMEs at the Earth can be potentially geoeffective depending on their dynamical and magnetic properties [*Lin et al.*, 1998]. The first arrival of the leading edge of the IP ejecta such as EJ or MC is used as the identification of the CMEs at the Earth.

[5] There has been the long-standing controversy about the relationship among metric type II bursts, flares, CMEs and IP shocks [*Chao*, 1974, 1984; *Wagner and McQueen*, 1983; *Gosling*, 1993; *Gosling and Hundhausen*, 1995; *Svestka*, 1995; *Dryer*, 1996; *Gopalswamy et al.*, 1998; *Cliver et al.*, 1999]. The one-shock versus the two-shock scenario was first suggested by *Chao* [1974, 1984], who argued that flare-generated shocks are easily dissipated and CME-generated shocks can last for a longer lifetime because the latter ejecta, or CMEs, can be maintained strong enough to generate IP shocks. *Gopalswamy et al.* [1998] proposed that metric type II bursts are produced by flares and then supported the idea that the metric type II shocks (coronal shocks) and deca-hectometric (D-H) type II shocks (IP shocks) are of independent origin as also suggested by *Wagner and McQueen* [1983]. *Gopalswamy et al.* [1998] reported that 93 metric type II bursts did not have IP signatures using the data from November 1994 to June 1998. On the other hand, *Cliver et al.* [1999] insisted that metric type II, EIT wave, and D-H type II bursts are driven by fast CMEs. The recently observed EIT waves are found to be associated with metric type II bursts [*Klassen et al.*, 2000; *Gopalswamy et al.*, 2000a] in their speeds and positions as well as with CMEs [*Thompson et al.*, 2000]. A theoretical three-dimensional (3-D) magnetohydrodynamics (MHD) model [*Wu et al.*, 2001] demonstrated that a pressure pulse (mimicing a flare) successfully reproduced the basic features of the 12 May 1997 EIT wave as well as the formation of local shocks and a density enhanced structure that resembled the upwardly moving CME in the corona. Recently, *Reiner et al.* [2001] suggested that the harmonic component of metric type IIs can be possibly related with D-H type IIs. Also, *Leblanc et al.* [2001] argued from 10 type II bursts that the shock waves may be driven by the CMEs all the way from $\sim 1 R_{\odot}$ to 1 AU. In addition, they admitted for some events that the evidence available cannot exclude the hypothesis that the shock is a blast wave from the flare to 1 AU [*Smart and Shea*, 1985]. *Cho et al.* [2003] reported that CMEs and flares are initiated nearly simultaneously, at least for type II associated events, based upon the temporal relationship obtained from data from May 1998 to December 2000.

[6] There are two kinds of models for the prediction of the solar disturbance arrival at the Earth: (1) empirical CME propagation models [*Gopalswamy et al.*, 2000b, 2001, 2003] and (2) ensemble of physically based shock propagation models [*Fry et al.*, 2003]. The empirical CME propagation models use initial plane-of-sky CME speeds for prediction of ICME (MC or EJ) and IP shock at 1 AU. The physical background assumed by the CME propagation models is that a flare-associated coronal shock, detected by the metric type II burst, will decay to a MHD wave close to the Sun. This view maintains that a separate, unspecified event will produce a CME that will produce its own shock that, in turn, will propagate ahead of it to IP space. This is basically the two (mutually independent)-shock scenario. On the other hand, the ensemble of shock propagation models uses coronal shock speeds from solar metric type II radio data for prediction of the shock arrival at the Earth. The shock propagation models are based on the one-shock scenario that metric type II shocks, flares, and deca-hectometric type II shocks can be directly related to in situ shock and storm sudden commencement (SSC) events.

[7] Even though these models show the different propagation (mass and shock) for different pairs of event (i.e., CME-ICME, CME-IP shock, and coronal shock-IP shock), it would be meaningful to compare the difference between estimated and observed arrival times of IP shocks and ICMEs for near-simultaneous CME and metric type II events. For this, we have considered 38 type II-CME events among the 173 type II solar events studied by *Fry et al.* [2003] according to their temporal and spatial proximity. Then we apply two types of prediction models to these events. The purpose of this paper is not only to compare the prediction accuracy but also to discuss their usefulness as prediction tools in terms of real-time forecasts, identification of arrival time, more successful alarms, etc. In section 2, we briefly describe the ensemble of shock propagation models such as STOA, ISPM, HAFv.2, STOA-2, and the empirical CME propagation models. We explain our data and analysis of the selected 38 CME-type II events in section 3. The predictability of the ensemble of the physically based shock propagation models and the empirical CME propagation models is compared in section 4. A brief summary and discussion are given in section 5.

2. Models

2.1. Ensemble of Shock Propagation Models

2.1.1. Shock Time of Arrival Model: STOA

[8] STOA is based on the theoretical concept of self-similar blast waves modified by the piston-driving idea and empirical shock shape in the ecliptic plane [*Dryer and Smart*, 1984; *Smart et al.*, 1984; *Smart and Shea*, 1985; *Lewis and Dryer*, 1987]. The initial explosion (flare) drives a shock. The shock is assumed to be initially driven at a constant speed, Vs, for a specified length of time (using GOES X-ray duration as a proxy) as discussed by *Smith et al.* [1994]. The shock then decelerates as a blast wave (where $Vs \sim R^{-1/2}$ and R is the heliocentric radius) as it expands outward. Required observational data are as follows: flare's heliolongitude, start time of the metric type II radio drift, the initial shock speed, the proxy piston driving time duration, and the L1 solar wind speed, Vsw, at approximately the time of the flare. Detailed descriptions of the model are well presented by several authors [e.g., *Dryer and Smart*, 1984; *Smart and Shea*, 1985; *Smith et al.*, 2000; *Fry et al.*, 2001].

2.1.2. A Revised STOA Model: STOA-2

[9] Noting the observational and numerical finding that the radial velocity of shock waves depends on the initial shock velocity, *Moon et al.* [2002a] suggested a simple modified STOA model (STOA-2) which has a linear relationship between the initial coronal shock wave velocity (V_{is}) and its deceleration exponent(N), $N = 0.05 + 4 \times 10^{-4} V_{is}$, where V_{is} is a numeric value expressed in units of km s^{-1}. They showed that the STOA-2 model not only removes a systematic dependence of the transit time differ-

ence predicted by the previous STOA model on initial shock velocity but also reduces the number of events with large transit time differences. Input parameters of the STOA-2 model are the same as those of the STOA model.

2.1.3. Interplanetary Shock Propagation Model: ISPM

[10] The ISPM is based on a parametric study of 2.5-D MHD simulations [*Smith and Dryer*, 1990]. Those calculations used a range of input shock speeds, temporal durations, and longitudinal widths (at the Sun) to mimic the solar flare over a range of helio-longitudes relative to the Earth's location. This study showed that the propagation of the resulting shock waves primarily depends upon the net input energy. If the net energy ejected into the solar wind by a solar source and the source's longitude are known, then the transit time to, and the strength of the shock at 1 AU may be computed from algebraic equations given by *Smith and Dryer* [1995]. This model also gives an estimate of the shock strength that is used as an indicator of confidence in the prediction. *Smith and Dryer* [1995] described the details of this model and the functions in the energy-longitude space.

2.1.4. Hakamada-Akasofu-Fry SolarWind Model: HAFv.2

[11] The HAF (version 2) is a ''modified kinematic'' solar wind model. ''Kinematic'' means that the model kinetically projects the flow of the solar wind from inhomogeneous sources near the Sun out into IP space. ''Modified'' means that the model adjusts the flow for stream-stream interactions as faster streams overtake slower ones. The model has important advantages over the other shock propagation models by providing a global picture of multiple and interacting shocks that propagate into nonuniform, stream-stream interacting solar wind flows. The input data to the model are similar to those used by the STOA and ISPM models as provided by the real-time observations discussed earlier. The HAFv.2 calculates solar wind speed, density, magnetic field, and dynamic pressure as a function of time and location. The model also gives an estimate of the confidence of predictions via a temporal stepwise calculation of a ''Shock Searching Index'' which is the logarithm (base 10) of the normalized dynamic pressure jump along the nonuniform shock surface. A detailed description of this model is given by *Hakamada and Akasofu* [1982] and *Fry et al.* [2001].

2.2. Empirical CME Propagation Models

2.2.1. CME-ICME Model

[12] Under the assumption that the speed of a CME changes between the Sun and the Earth due to the drag exerted by the solar wind on the CME, *Gopalswamy et al.* [2000b] presented an empirical model for CME propagation which is able to predict how much time it takes for a CME to travel the distance between the Sun and the Earth. *Gopalswamy et al.* [2001] improved their model and evaluated the prediction capability of the model for 47 CME events, 19 of which were labeled with question marks for their ICME counterparts [*Gopalswamy et al.*, 2001, Table 2]. They found that the CMEs are first subjected to an IP acceleration and then allowed to propagate freely beyond an acceleration-cessation distance (0.76 AU). The mean error of the model corresponding to the acceleration-cessation distance was presented as 10.7 hours. The model is in good agreement with the observations for high-speed CMEs ($u > 600$ km s^{-1}). However, the agreement is not so good for low-speed events; this fact was attributed to the likelihood that slow CMEs might stop accelerating before reaching 0.76 AU [*Gopalswamy et al.*, 2001].

2.2.2. CME-IP Shock Model

[13] *Gopalswamy et al.* [2003] extended the CME-ICME model to predict IP shock arrivals at the Earth by using the gas dynamic, one-dimensional, time-dependent (shock-tube), piston-shock relationship [*Landau and Lifshitz*, 1987] between the piston speed and the speed of the shock ahead of the CME for the limiting case of infinite sonic Mach number. To obtain the shock arrival time (SAT), they considered the position of the piston for the CME to be at 0.5 AU and derived the standoff distance between the leading edge of the MC and the shock by using an empirical relationship for the two-dimensional, steady-state, solid body-bow shock standoff distance. The standoff distance is then used to obtain the SAT by shifting the CME arrival time in accordance with the distance. They analyzed a set of 29 IP shocks and the associated MCs observed by the WIND spacecraft and concluded that the piston-shock relationship holds.

3. Selection of Events

[14] The accuracy of STOA and ISPM was first evaluated in a real-time forecast study [*Smith et al.*, 2000]. Recently, *Fry et al.* [2003] compared the performance of the HAFv.2 model with the performances of the STOA and ISPM models for 173 metric type II events during the rise of solar maximum from February 1997 to October 2000. Their statistical comparison between the models showed them to be practically equivalent in predicting SAT. The uncertainty of the SAT estimates as determined by RMS error is about 12 hours for each model. On the other hand, *Gopalswamy et al.* [2001] applied the CME-ICME propagation model to 47 CME events observed from December 1996 to July 2000 by SOHO. Then they showed that the average prediction error of the model is 10.7 hours. *Gopalswamy et al.* [2003] extended the CME-ICME model to predict 1 AU arrival of IP shocks as discussed in section 2.2.2. They used a set of 29 IP shocks and the following ICMEs observed by WIND spacecraft from January 1997 to May 2002 and concluded that empirically shifting the CME-ICME model by an interval corresponding to the gas dynamic bow shock standoff distance provided a simple, however physically inconsistent, means of estimating the shock arrival time.

[15] The prediction errors of these models are not conclusive because these values are obtained from different data sets. Recently, it has been suggested that CMEs and flares (metric type II) are initiated nearly simultaneously [e.g., *Zhang et al.*, 2001; *Neupert et al.*, 2001; *Moon et al.*, 2002b; *Cho et al.*, 2003; *Shanmugaraju et al.*, 2003]. Therefore it would be meaningful to compare the prediction errors of the above two types of models for near-simultaneous CME-metric type II events. Thus we select the CMEs that have the temporal and spatial proximity to the type II events in Table 1 of *Fry et al.* [2003]. For this, we use the first C2 appearance time, position angle, and linearly fitted speeds of the CMEs that were adopted from SOHO/LASCO CME Catalog of CSPSW/NRL (available at http://cdaw.gsfc.nasa.gov/CME_list/). The errors of the CME speeds are known by their experience to be typically 10% but sometimes 30% (S. Yashiro, private communication, 2002).

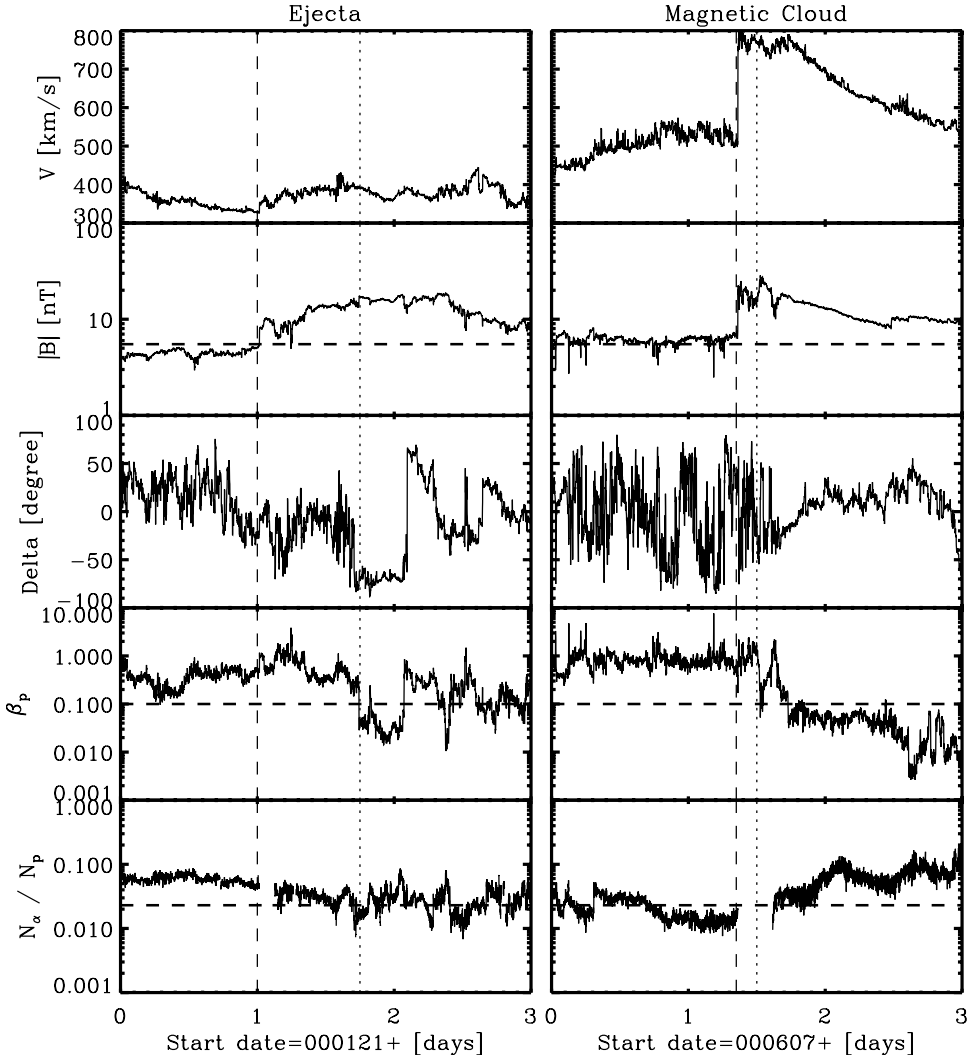

Figure 1. Representative examples of observed IP shock and ICME event at 1 AU as measured by the ACE spacecraft. The left vertical dashed line indicates the arrival time of the IP shock and the right dotted line denotes the arrival time of ICME. Dashed lines across each panel indicate the value of 5.5 nT ($|B|$), 0.1 (β_p), 2.3% (N_α/N_p) as ICME signatures for either Ejecta (EJ) or Magnetic Cloud (MC).

[16] The procedure for examining the arrival time predictions of ICMEs and IP shocks for the near-simultaneous events are summarized as follows: (1) From the 173 type II events of *Fry et al.* [2003], we choose a total of 101 CMEs that are within a threshold window (±90 min). (2) We select 89 events from this group by comparing the position angles and the coordinate information of the associated flares. (3) We apply the adopted prediction models (the ensemble of shock propagation models and the empirical CME propagation models) to the selected events. Then we look for IP shocks that appear near the predicted times. For this, we examine the IP shocks identified by *Fry et al.* [2003] who used the NOAA/SEC 1-min resolution ACE and/or WIND plasma and field data, searching for simultaneous jumps in velocity, density, temperature, and total magnetic field magnitude according to the Rankine-Hugoniot relations. As a result, we identified 38 IP shocks. (4) We then search for ICMEs associated with the 38 IP shocks. For the identification of ICMEs, we look for MC and EJ from in situ magnetic field-plasma measurements and particle detection of ACE (available at http://www.srl.caltech.edu/ACE/ASC/level2/index.html). According to *Burlaga* [1995] and *Berdichevsky et al.* [2002], a MC is defined as a large flux-rope structure of an almost cylindrical shape with low plasma beta (<0.1), high alpha/proton ratios (>0.6), enhanced magnetic field strength (>10 *nT*), and a large and smooth rotation of the magnetic field direction. In the case of EJs, which are not flux ropes and have disordered magnetic fields, smooth rotation may not be present. We also refer to previously identified sources of ICMEs [*Gopalswamy et al.*, 2001; *Cane and Richardson*, 2003] and the Magnetic Cloud Table (available at http://lepmfi.gsfc.nasa.gov/mfi/mag_cloud_pub1p.html).

[17] Figure 1 presents typical observations of EJ (left panels) and MC (right panels) showing signatures of IP shocks and ICMEs. Starting from the top, the first panel contains the solar wind speed as measured by the ACE spacecraft. The second panel presents the magnitude of magnetic field. The horizontal dashed line in this panel indicates the historical value of 5.5 nT that supposedly

Table 1. Solar Disturbances and Their Arrivals at L1

Event	Solar Disturbances					Arrival Time	
No.[f]	Date/UT (CME)	P.A.[a]	V_{CME} (km/s)	$V_{type\ II}$ (km/s)	ΔT_{CT}[b] (min)	Date/UT[c] (Shock)	Date/UT[d] (ICME)
2	970407/1427	Halo	830	800	29	0410/1258	0411/0600(E)
3	970512/0630	Halo	464	1400	74	0515/0115	0515/1000(M)
5	971104/0610	Halo	785	1400	2	1106/2218	1107/0530(M)
6	971127/1357	98	441	700	40	1130/0714	–
22	981105/2059	Halo	1124	900	68	1108/0420	1108/0900(M)
38	990209/0533	235	808	600	14	0211/0858	–
44	990308/0654	115	664	700	16	0310/0038	–
55	990622/1854	Halo	1133	1400	30	0626/0217	0626/0500(E)
57	990629/0554	Halo	589	750	39	0702/0025	–
60	990711/0131	81	318	650	78	0713/0845	–
62	990719/0306	Halo	430	500	50	0722/0950	–
70	990804/0626	262	405	462	34	0808/1750	0809/1048(E)
74	990820/2326	95	812	700	9	0823/1130	–
78	990828/1826	120	462	600	19	0831/0131	–
79	990830/0850	9	404	700	47	0902/0935	–
80	990913/1731	109	444	500	69	0915/2005	–
97	991222/0230	Halo	570	500	29	1226/2126	1227/1800(E)
102	000118/1754	Halo	739	400	35	0122/0023	0122/1800(E)
104	000208/0930	Halo	1079	600	33	0211/0213	0211/1000(M)
105	000210/0230	Halo	944	1100	42	0211/2318	0212/1500(M)
106	000212/0431	Halo	1107	700	25	0214/0656	0215/0000(M)
108	000217/2130	Halo	550	550	66	0220/2050	0221/0948(E)
129	000430/0854	186	540	700	49	0502/1044	–
130	000510/2006	83	641	680	28	0512/1712	0514/0300(M)
133	000520/0626	187	557	500	30	0523/2315	–
135	000606/1554	Halo	1119	1189	31	0608/0840	0608/1200(M)
136	000607/1630	Halo	842	826	40	0611/0716	0611/0900(E)
140	000615/2006	298	1081	996	20	0618/1702	–
142	000618/0210	307	629	660	12	0621/1500	–
151	000710/2150	67	1352	1300	27	0713/0918	–
152	000712/2030	281	820	950	16	0714/1532	0715/0600(M)
153	000714/1054	Halo	1674	1800	34	0715/1437	0715/2200(M)
158	000722/1154	304	1230	1000	29	0725/1322	–
159	000725/0330	Halo	528	903	41	0728/0541	0728/1500(E)
165	000901/1854	244	411	500	27	0906/1612	0907/0400(E)
169	000916/0518	Halo	1215	773	45	0917/1657	0918/0100(M)
171	001001/1350	94	427	1100	38	1003/0007[e]	1005/1200(M)
172	001009/2350	Halo	798	925	12	1012/2144	1013/1700(M)

[a]Position angles of CMEs.
[b]Time difference between the first CME appearance and the starting of type II bursts.
[c]Observed shock arrival date and time at L1.
[d]Observed CME arrival date and time at L1. M denotes Magnetic cloud and E, Ejecta.
[e]ICME associated IP shock which was observed at 1005/0241 (UT).
[f]Event numbers are taken from the metric type II/flare events in the work of *Fry et al.* [2003].

"defines" the occurrence of an ICME when taken with the other parameters [*Berdichevsky et al.*, 2002]. The third panel presents the latitude of the magnetic field in the spacecraft-centered coordinate system. The fourth panel shows the proton plasma beta (β_P), and the bottom panel is the ratio of alpha particle to proton density, N_α/N_P. A dashed line across the N_α/N_P panel gives 2.3% which is the approximate mean value of this density ratio [see, e.g., *Berdichevsky et al.*, 2002]. While large ICMEs obviously satisfy the definitions suggested by *Burlaga et al.* [1981], small ones have many small and less obvious structures. The uncertainty in determination of the ICME's leading edge can be several hours for different criteria. On the basis of these observational criteria, we have identified 22 ICME events. It is noted that most of the ICMEs (17/22 or 77%) originated from halo CMEs, which is consistent with the results of *Gopalswamy et al.* [2003].

[18] Table 1 shows the details of the 38 near-simultaneous CME-type II burst events that are followed by IP shocks and/or ICMEs. The first six columns give the type II burst

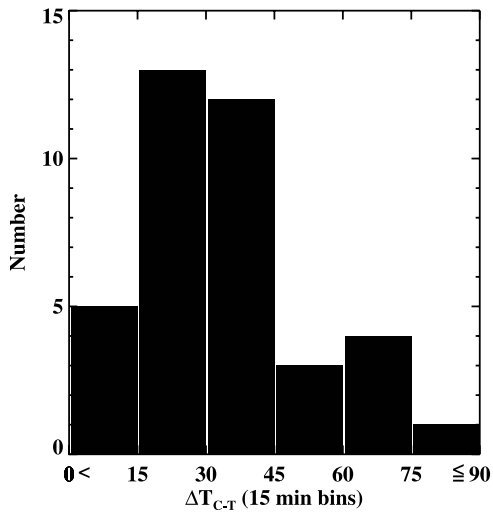

Figure 2. Histogram showing time difference between the first appearance of CME and the starting of the type IIs.

Table 2. Transit Times of Shock and ICME and the Discrepancies Between Prediction and Observation for Each Model

Event	Transit Time			Prediction Difference					
No.	TT_S[a] (hr)	TT_C[b] (hr)	ΔT_{SI}[c] (hr)	ΔT_G[d] (hr)	ΔT_{G2}[e] (hr)	ΔT_S[f] (hr)	ΔT_{S2}[g] (hr)	ΔT_I[h] (hr)	ΔT_H[i] (hr)
2	71	87.5	−17.0	−10.9	−11.4	0.1	−3.8	2.1	−11.0
3	68	75.5	−8.75	26.9	17.0	−22.2	−9.8	−38.5	−31.3
5	64.2	71.3	−7.2	9.7	−1.6	−12.3	−3.0	−24.2	−23.3
6	65.9	–	–	–	–	20.8	12.5	–	−21.8
22	56.5	60.1	−4.6	−7.0	−13.9	6.6	3.8	0.3	−2.3
38	51.7	–	–	–	–	32.5	17.9	–	7.0
44	42	–	–	–	–	32.0	27.8	–	52.4
55	79.9	82.1	−2.71	−31.6	−38.3	−26.9	−9.6	−40.9	−37.3
57	67.2	–	–	–	–	−1.2	−3.6	14.8	−7.4
60	56.5	–	–	–	–	51.5	39.4	–	17.3
62	79.6	–	–	–	–	10.4	−3.6	8.4	−12.9
70	108	124.3	−16.9	−20.9	−21.4	mhd**	−20.6	mhd	–
74	60.2	–	–	–	–	8.8	5.5	–	54.5
78	55.4	–	–	–	–	2.6	−7.5	16.6	−5.5
79	63.5	–	–	–	–	−7.5	−10.2	−1.5	−0.5
80	51.7	–	–	–	–	10.3	3.3	48.3	3.9
97	115.4	135.5	−20.56	−36.8	−36.6	−15.4	−33.0	–	−38.4
102	79.1	96.1	−17.6	−10.5	−12.4	mhd	−0.4	mhd	1.6
104	65.3	72.5	−7.78	−16.6	−21.0	−4.3	−9.1	10.7	22.7
105	45.5	60.5	−15.7	5.6	6.5	6.5	7.4	−5.5	7.7
106	50.8	67.5	−19.5	−13.4	−5.7	6.2	1.6	27.2	17.1
108	72.4	84.3	−12.9	15.3	8.1	−8.4	−19.1	0.6	−11.8
129	50.6	–	–	–	–	17.4	11.7	12.4	−6.7
130	45.6	78.9	−33.8	15.2	28.4	28.4	21.6	18.4	16.8
133	89.3	–	–	–	–	−14.3	−25.7	10.7	−18.2
135	41.3	44.1	−3.3	9.2	0.96	7.7	10.5	−3.3	−4.7
136	87.4	88.5	−1.73	−12.0	−28.5	−30.4	−34.0	−28.4	−34.2
140	69.3	–	–	–	–	−17.3	−17.4	18.7	5.9
142	85.0	–	–	–	–	mhd	−0.3	mhd	15.0
151	59.9	–	–	–	–	−13.9	−5.9	−14.9	−8.3
152	43.3	57.5	−14.4	20.15	16.8	21.7	21.8	mhd	41.5
153	28.3	35.1	−7.3	−3.35	−2.33	0.7	31.5	−3.3	−0.6
158	73.9	–	–	–	–	−9.9	−9.5	mhd	−3.3
159	74.9	88.5	−9.3	17.07	6.49	5.1	5.8	−6.9	−25.7
165	117.8	129.1	−11.8	−25.7	−31.4	mhd	−42.5	mhd	−0.2
169	36.4	43.7	−8.05	4.18	2.0	30.6	24.9	23.6	12.1
171	34.9 (84.9[j])	94.17	−59.3 (−9.3[j])	8.98	(0.4[j])	19.1	20.5	6.1	8.9
172	70.1	89.2	−19.26	−9.34	−8.3	−13.1	−13.4	−24.1	−13.7

[a,b]Transit time of observed IP shock and ICME.
[c]Time lag between IP shock and ICME.
[d,e]Predicted - observed transit time for the CME-ICME model and the CME-IP shock model. The subscripts G and G2 refer to the procedures given by *Gopalswamy et al.* [2001] and *Gopalswamy et al.* [2003], respectively.
[f,g,h,i]Predicted transit time minus observed transit time for STOA, STOA-2, ISPM, and HAFv.2, respectively.
[j]Derived by using the ICME associated with the IP shock observed at 001005/0241 (UT).
[k]mhd: indicates that the specific model (here, STOA and ISPM) predicted that the portion of the shock that was headed toward Earth had decayed to an MHD wave prior to reaching this position.

event number from *Fry et al.* [2003], the first CME appearance (time) in the C2 image, the position angle of the CME measured counterclockwise in degrees from solar north, the linearly fitted speed of the CME, the mean speed of the type II radio burst, and the difference between the first C2 appearance time and the starting time of the type II burst, respectively. All CME information is taken from the SOHO/LASCO CME Catalog of CSPSW/NRL, and the details of the type IIs can be found in Table 1 of *Fry et al.* [2003]. The seventh and eighth columns represent the arrival times of the shocks and the ICMEs at 1AU, respectively.

4. Results

[19] Figure 2 is a histogram showing the difference between the first appearance time of the CMEs in the LASCO C2 field-of-view (taken as the "starting" time of the CMEs) and the starting time of the type IIs for the selected 38 events. In all cases, the type II onset occurred prior to the CME appearance in the LASCO images. Their mean time difference is 35 min. The average speeds of the CMEs and the type IIs are 762 km s^{-1} and 827 km s^{-1}, respectively.

[20] By applying the adopted prediction models to the selected type II-CME events and using the arrival times of IP shocks and ICMEs, we estimated the difference between the predicted time and the observed time for each model. In Table 2, the first four columns give the event number from *Fry et al.* [2003] and the transit times of IP shocks and ICMEs from the Sun to the Earth and the time lags between IP shock and ICME arrivals. The $\Delta T's$ in the latter six columns are the time differences between predicted transit times by the adopted models and observed ones for the shocks and ICMEs. All of the 22 identified ICMEs are preceded by IP shocks as shown in Table 2. The mean time interval between the shock arrival and the arrival of the trailing ICME at the Earth is about 12 hours, which is comparable to the estimates of *Berdichevsky et al.* [2002].

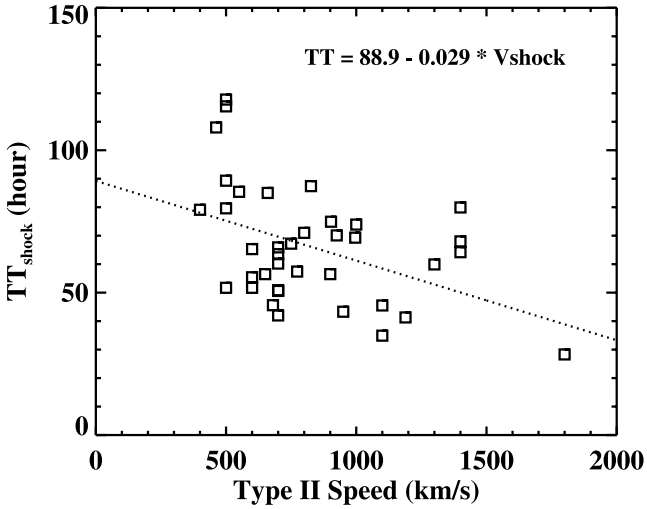

Figure 3. Metric type II speed (V_s) versus the transit time (TT_{shock}) of IP shocks. The dashed line is a straight-line fit to the data points.

[21] Figure 3 shows the IP shock transit time as a function of the corresponding coronal shock speed along with a straight line fit to the scattered data. It ranges from 28 to 118 hours with a mean value of 66 hours. There is an approximate linear trend that a fast coronal shock has a short transit time, as would be expected, regardless of the heliolongitude of its solar source. In Figure 4, we plot the transit time of observed ICMEs (diamonds) and IP shocks (crosses) for the 22 events as a function of CME speed. The difference between the number of solar-observed CMEs (38) and IP-observed ICMEs (22), by the criteria discussed above, is probably due to the likelihood of the higher collimation, thus avoiding Earth encounter of the MCs or EJs from solar sources located far from central meridian.

[22] In order to examine in more detail the relationship between the initial speeds and transit times of shocks and

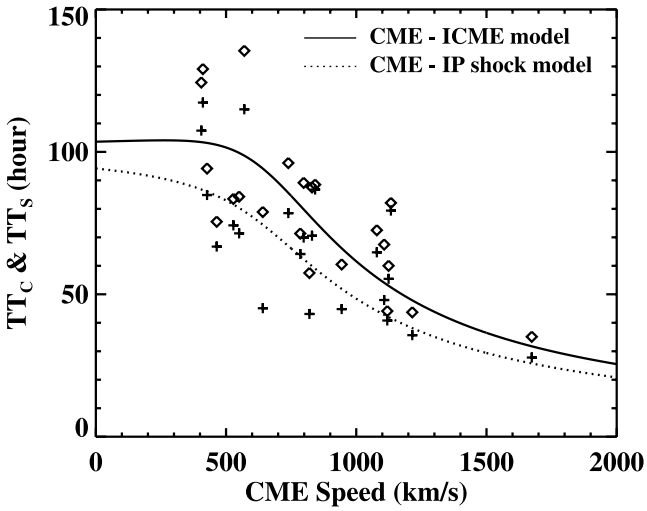

Figure 4. Initial speed of CMEs vs the transit time of ICMEs (TT_C) and IP shocks (TT_S). The solid and dotted lines denote the CME-ICME model and the CME-IP shock model, respectively. Crosses indicate observed shocks, and diamonds indicate observed ICMEs.

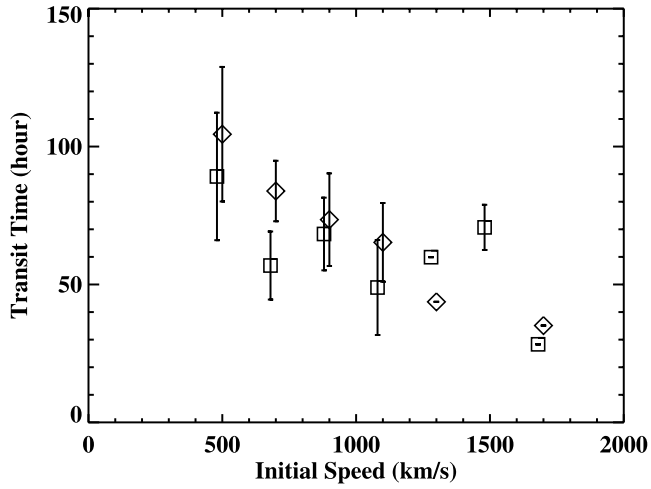

Figure 5. Mean transit time of IP shocks (squares) and ICMEs (diamonds) as a function of their initial speed, i.e., the coronal shock speed and the CME speed in LASCO field of view. The error bars are the mean standard deviations within a speed window of 200 km s^{-1}.

CMEs, we present mean transit times within a speed window of 200 km s^{-1} and their errors in Figure 5. As seen in the figure, the transit time of an CME is more dependent on its initial CME speed than that of an IP shock on the coronal shock speed.

[23] The number of events that are predicted by the shock and CME propagation models within an arbitrarily chosen window of ±60 hours are 34 (STOA), 38 (STOA-2), 26 (ISPM), 37 (HAFv.2), and 22 (empirical CME propagation models), respectively. Figure 6 shows histograms of the time differences for the ensemble of shock propagation models. Their statistical results are summarized in Table 3, where three time windows (12 hours, 24 hours, and 60 hours) for correct prediction are adopted to derive their mean and RMS errors. As seen in Table 3, the prediction errors and success rates of the STOA, STOA-2, ISPM, and HAFv.2 models are comparable to one another. The average error for all models within ±24 (12) hours is about 9.8 (5.6) hours. Their success rates are about 80% for the 24-hour window and 50% for the 12-hour window. Figure 7 presents the time difference between predicted and observed for the empirical CME propagation models. The CME-ICME model predicts 18 (11) of the 22 events within ±24 (12) hours, and their mean error is 11.6 (7.8) hours. These statistical results are also listed in Table 3 and compared with the other models. The derived mean error of the CME-ICME model is comparable not only with that (10.7 hours) of *Gopalswamy et al.* [2001] but also with those of the shock arrival models. The CME-IP shock model predicts 17 (11) of the 22 events within ±24 (12) hours and their mean error is 9.2 (4.9) hours. As seen in Table 3, statistical results strongly depend on an adopted window. When the window is reduced from ±24 hours to ±12 hours, the ICME prediction error becomes bigger than the average of the shock prediction error, which might be attributed to the uncertainty of ICME arrival identification as discussed earlier.

[24] In all the histograms except the result of the STOA-2 model, the plots in Figure 6 and Figure 7 do not have normal distributions, and each model shows different error patterns.

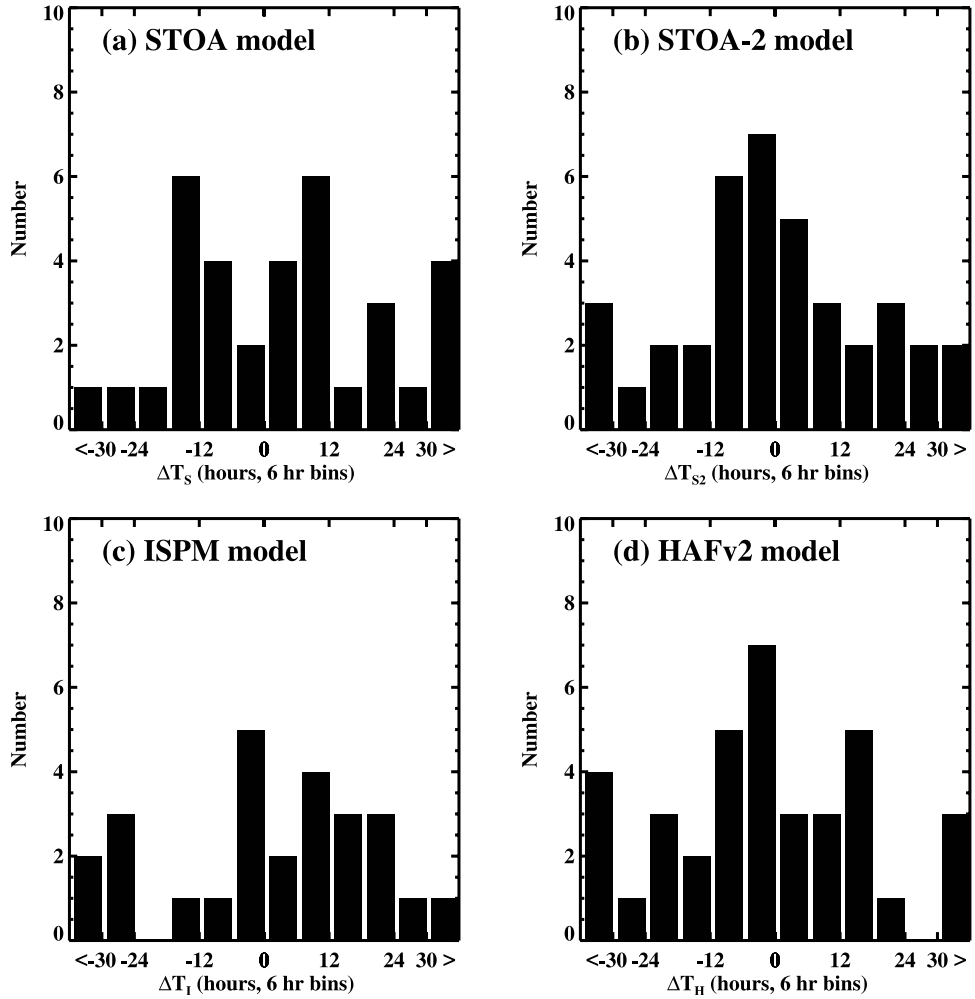

Figure 6. Histograms showing the time difference between predicted and observed for the ensemble of shock propagation models using 6-hour bins. Transit time difference ΔT_P (= $TT_P - TT_S$) is based on the STOA, STOA-2, ISPM, and HAFv.2 models.

If the shock and CME propagations are mainly accounted for by these models and affected additionally by other minor factors, the number distribution of transit time differences would follow a normal distribution with a peak around zero. However, we have several error sources such as assumed coronal density distribution, plane-of-sky speed of CME, complex heliospheric environments, and solar wind inhomogeneities [*Aubier et al.*, 1986; *Moon et al.*, 2002a]. These error sources may not be minor for some cases and can result in complex distributions of transit time differences. By examining the discrete pattern of the transit time differences for the STOA and STOA-2 models, *Moon et al.* [2002a] suggested that inhomogeneous density distributions in the solar corona are a plausible near-Sun origin for the transit time difference. Thus our judgment is reserved for further studies using more extended data samples and improved 3-D MHD propagation models [cf. *Dryer*, 1994].

5. Summary and Discussion

[25] In this paper, we have compared the prediction capability of two types of Sun-Earth connection models: (1) ensemble of shock propagation models (STOA, STOA-2, ISPM, and HAFv.2) and (2) empirical CME propagation (CME-ICME and CME-IP shock) models. For this objective, we have applied these models to 38 near-simultaneous CME-metric type II burst events. That is, these events can reasonably be taken to be associated with specific solar flares as given by *Fry et al.* [2003]. Major results from this study can be summarized as follows:

[26] 1. The mean time difference between the first CME appearance in the LASCO C2 field of view and the starting

Table 3. Number of Correct Predictions and the Prediction Errors for Each Model

	STOA	STOA-2	ISPM	HAFv.2	CME-ICME	CME-IP
No.($\leq\pm60h$)	34	38	26	37	22	22
RMS(ΔT)	18.9	18.3	20.3	21.6	17.3	18.6
Mean(ΔT)	14.5	14.4	15.8	16.3	15.0	14.5
No.($\leq\pm24h$)	27(77%)	30(76%)	19(73%)	29(78%)	18(81%)	17(77%)
RMS(ΔT)	12.8	11.7	11.6	12.0	12.6	11.4
Mean(ΔT)	10.5	9.7	9.4	9.9	11.6	9.2
No.($\leq\pm12h$)	16(46%)	21(53%)	12(46%)	18(49%)	11(50%)	11(50%)
RMS(ΔT)	6.9	6.9	6.1	6.4	8.7	6.0
Mean(ΔT)	6.0	6.0	5.0	5.4	8.2	4.9

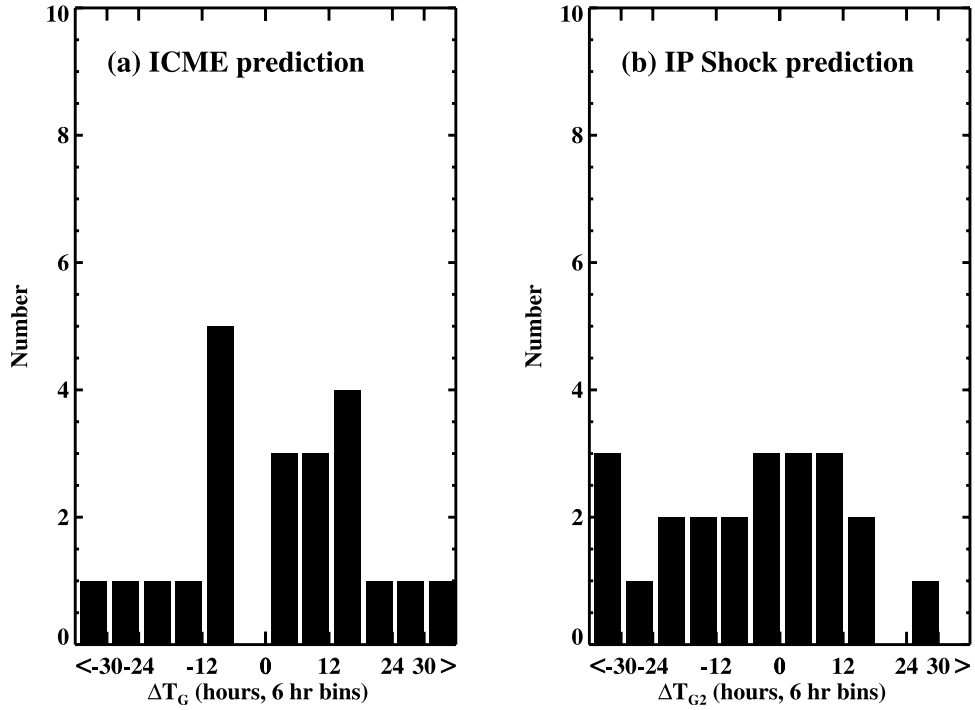

Figure 7. Histograms showing the time difference between predicted and observed for the empirical CME propagation models using 6-hour bins. Transit time differences (ΔT_G and ΔT_{G2}) are derived by the CME-ICME model and the CME-IP shock model, respectively.

time of type II bursts for the selected events is found to be 35 min. The average speeds of the CMEs and the metric type IIs are 762 km s^{-1} and 827 km s^{-1}, respectively. These results are consistent with recent results of *Shanmugaraju et al.* [2003] and *Claßen and Aurass* [2002] who studied the association between type II radio bursts and CMEs during the last solar maximum period 1999–2001.

[27] 2. Most of the identified ICMEs are preceded by IP shocks. The mean time difference between the IP shock and ICME arrivals at the Earth is about 12 hours, which is consistent with previous results [e.g., *Berdichevsky et al.*, 2002; *Oh et al.*, 2002; *Cane and Richardson*, 2003; *Gopalswamy et al.*, 2003].

[28] 3. The estimated mean error of the shock arrival time (SAT) within an adopted window of ±24 hours is 9.8 hours for the ensemble of shock propagation models, 9.2 hours for the CME-IP shock model, and 11.6 hours for the CME-ICME model.

[29] 4. The success rates are found to be about 80% for the adopted window of ±24 hours and comparable to one another. There are 20% of cases where the predictions exceed 24 hours in errors. We can think of four possible reasons for this large uncertainty as follows. (1) There are shock speed errors that originated from the assumed coronal density. In fact, coronal density is quite inhomogeneous (e.g., helmet streamer and coronal hole). Regarding this, *Sun et al.* [2002] suggested that a 3-D MHD coronal density model should be developed for time-specific and location-specific solar flares and their associated type II radio burst and/or CME observations. (2) CME speeds have projection effect uncertainties that can result in underestimations. For example, *Gopalswamy and Kaiser* [2002] argued, from radio observations, that the plane-of-sky speed of a particular halo CME was smaller than the speed in the direction of the Earth by at least a factor of two for a centrally located flare eruption. (3) There may be complex heliospheric environments such as shock-shock, shock-ICME, and ICME-ICME interactions. (4) We might have made some misidentifications (i.e., wrong linkage between the solar source and the IP consequence).

[30] Summing up, the predictability of two types of the Sun-Earth connection models is comparable to each other in terms of their prediction errors. In addition, their prediction capability may be discussed in the following several aspects. First, both types of models can, obviously, be used for real-time forecasts of solar disturbances. In fact, the ensemble of the shock propagation models has been employed in real-time to predict the arrival time of IP shocks using type II burst data for a few years (e.g., http://www.expi.net/expinet/tools.html). A similar type of prediction may be possible for the CME propagation models since near real-time data of CMEs (e.g., SOHO/LASCO) are available. If all CMEs are considered in these models, there would be numerous false alarms. To avoid such false alarms, some procedures to select geoeffective CMEs are required (e.g., halo CMEs). In addition, a predictability test based on a contingency table [e.g., *Smith et al.*, 2000; *Fry et al.*, 2003] would be meaningful. Second, while the shock propagation models are based on the one-shock scenario whereby a sufficiently strong coronal shock propagates into the heliosphere and arrives at the Earth, the CME propagation models are based on the premise of the two-shock scenario and empirical relationships between kinematic parameters. Also, the latter models make no provision for noncircular shock or ICME shapes in the ecliptic plane. As discussed in the Introduction, the origins of coronal and IP

shocks are in debate. Thus further detailed investigations are required to compare the shock propagation models with the CME-IP shock model in terms of geoeffective origin and their underlying physics. Third, these models may be compared in terms of the identification of IP shock and ICME arrivals. In practice, the identification of IP shocks is much easier than that of ICMEs. The latter is highly subjective due to the fact that there are some ambiguities involved in the identification of ICME arrivals as discussed in section 3. We feel that both types of models (physics-based vis-a-vis empirical-based) can be complementary to each other in terms of practical forecasts of the arrival times of solar disturbances at the Earth. Finally, however, we also feel that future improvements in the understanding and global insight of the disturbances discussed here, as well as in their operational utilization, will be dependent on physics-based model developments.

[31] **Acknowledgments.** We are very thankful to the referees for their valuable comments. We thank G. Michalek and S. Yashiro very much for their help to identify the first C2 appearance times and heights of CMEs. We thank Z. Smith (NOAA Space Environment Center) for her constructive suggestions. This work has been supported by National Research Laboratory grant M10104000 059-01J000002500 of the Korean government and a MURI grant of AFOSR. MD and CDF acknowledge the support of the Geophysical Institute (University of Alaska at Fairbanks) under the DoD project, University Partnering for Operational Support (UPOS), and MD appreciates the hospitality of the NOAA Space Environment Center. MD and CDF also acknowledge partial support from the NASA's Living With a Star program. KSK thanks for the support of ABRL grant R14-2002-043-01000-0. The CME catalog we have used is generated and maintained by NASA and The Catholic University of America in cooperation with the Naval Research Laboratory. SOHO is a project of international cooperation between ESA and NASA.

[32] Lou-Chuang Lee thanks Jih Kwin Chao and another reviewer for their assistance in evaluating this paper.

References

Aubier, M. G., Y. Leblanc, and R. A. Howard, Non-constant apparent velocity of shock waves propagating in the altitude range of 1.2–2.6 solar radii, *Adv. Space Res.*, *6*, 315–318, 1986.

Berdichevsky, D. B., et al., Halo-corona mass ejections near the 23rd solar minimum: Lift-off, inner heliosphere, and in situ (1AU) signatures, *Ann. Geophys.*, *20*, 891–916, 2002.

Burlaga, L. F., *Interplanetary Magnetohydrodynamics*, Oxford Univ. Press, New York, 1995.

Burlaga, L. F., E. Sittler, F. Mariani, and R. Schwenn, Magnetic loop behind an interplanetary shock: Voyager, Helios, and IMP 8 observations, *J. Geophys. Res.*, *86*, 6673–6684, 1981.

Cane, H. V., and I. G. Richardson, Interplanetary coronal mass ejections in the near-Earth solar wind during 1996–2002, *J. Geophys. Res.*, *108*(A4), 1156, doi:10.1029/2002JA009817, 2003.

Chao, J. K., A model for the propagation of flare-associated interplanetary shock waves, in *Solar Wind Three*, edited by C. T. Russell, pp. 169–174, Inst. of Geophys. and Planet. Phys., Univ. of Calif., Los Angeles, 1974.

Chao, J. K., Some characteristics of propagation of flare- or CME-associated interplanetrary shock waves, *Adv. Space Res.*, *4*, 327–330, 1984.

Cho, K.-S., K.-S. Kim, Y.-J. Moon, and M. Dryer, Initial results of the Ichon solar radio spectrograph, *Solar Phys.*, *212*, 151–163, 2003.

Claßen, H. T., and H. Aurass, On the association between type II radio bursts and CMEs, *Astron. Astrophys.*, *384*, 1098–1106, 2002.

Cliver, E. W., D. F. Webb, and R. A. Howard, On the origin of solar metric type II bursts, *Solar Phys.*, *187*, 89–114, 1999.

Dryer, M., Interplanetary studies: Propagation of disturbances between the Sun and the magnetosphere, *Space Sci. Rev.*, *67*, 363–419, 1994.

Dryer, M., Comments on the origins of coronal mass ejections, *Solar Phys.*, *169*, 421–429, 1996.

Dryer, M., and D. F. Smart, Dynamical models of coronal transients and interplanetary disturbances, *Adv. Space Res.*, *4*, 291–301, 1984.

Fry, C. D., W. Sun, C. S. Deehr, M. Dryer, Z. Smith, S.-I. Akasofu, M. Tokumaru, and M. Kojima, Improvements to the HAF solar wind model for space weather predictions, *J. Geophys. Res.*, *106*, 20,985–21,002, 2001.

Fry, C. D., M. Dryer, Z. Smith, W. Sun, C. S. Deehr, and S.-I. Akasofu, Forecasting solar wind structures and shock arrival times using an ensemble of models, *J. Geophys. Res.*, *108*(A2), 1070, doi:10.1029/2002JA009474, 2003.

Gopalswamy, N., and M. L. Kaiser, Solar eruptions and long wavelength radio bursts: The 1997 May 12 event, *Adv. Space Res.*, *29*, 307–312, 2002.

Gopalswamy, N., M. L. Kaiser, R. P. Lepping, S. W. Kahler, K. Ogilvie, D. Berdichevsky, T. Kondo, T. Isobe, and M. Akioka, Origin of coronal and interplanetary shocks: A new look with WIND spacecraft data, *J. Geophys. Res.*, *103*, 307–316, 1998.

Gopalswamy, N., M. L. Kaiser, J. Sato, and M. Pick, Shock wave and EUV transient during a flare, in *High Energy Solar Physics Workshop—Anticipating HESSI*, *ASP Conf. Ser.*, vol. 206, edited by R. Ramaty and N. Mandzhavidze, p. 351, Astron. Soc. of the Pacific, San Francisco, Calif., 2000a.

Gopalswamy, N., A. Lara, R. P. Lepping, M. L. Kaiser, D. Berdichevsky, and O. C. St. Cyr, Interplanetary acceleration of coronal mass ejections, *Geophys. Res. Lett.*, *27*, 145–148, 2000b.

Gopalswamy, N., A. Lara, S. Yashiro, M. Kaiser, and R. A. Howard, Predicting the 1-AU arrival times of coronal mass ejections, *J. Geophys. Res.*, *106*, 29,207–29,218, 2001.

Gopalswamy, N., A. Lara, P. K. Manoharan, and R. A. Howard, An empirical model to predict the 1-AU arrival of interplanetary shocks, *Adv. Space Res.*, in press, 2003.

Gosling, J. T., The solar flare myth, *J. Geophys. Res.*, *98*, 18,937–18,950, 1993.

Gosling, J. T., and A. J. Hundhausen, Reply, *Solar Phys.*, *160*, 57–60, 1995.

Hakamada, K., and S.-I. Akasofu, Simulation of three-dimensional solar wind disturbances and resulting geomagnetic storms, *Space Sci. Rev.*, *31*, 3–70, 1982.

Kartalev, M. D., K. G. Grigorov, Z. Smith, M. Dryer, C. D. Fry, W. Sun, and C. S. Deehr, Comparative study of predicted and experimentally detected interplanetary shocks, in *Proceedings of the SOLSPA Euro Conference on Solar Cycle and Space Weather, 477, Vico Equense, Italy, 24–29 September 2001, ESA Publ.*, vol. 477, pp. 355–358, Eur. Space Agency, Paris, 2001.

Klassen, A., H. Aurass, G. Mann, and B. J. Thompson, Catalogue of the 1997 SOHO-EIT coronal transient waves and associated type II radio burst spectra, *Astron. Astrophys. Suppl. Ser.*, *141*, 357–369, 1997.

Landau, L. D., and E. M. Lifshitz, *Fluid Mechanics*, 2nd ed., Pergamon, New York, 1987.

Leblanc, Y., G. A. Dulk, A. Vourlidas, and J.-L. Bougeret, Tracing shock waves from the corona to 1 AU: Type II radio emission and relationship with CMEs, *J. Geophys. Res.*, *160*, 25,301–25,312, 2001.

Lepping, R. P., and J.-K. Chao, A shock surface geometry: The 15–16 February 1967 event, *J. Geophys. Res.*, *81*, 60–64, 1976.

Lewis, D., and M. Dryer, Shock-Time-of-Arrival model (STOA-87), NOAA/SEL Contract Rep. (Syst. Doc.) to U.S. Air Weather Serv., Natl. Ocean. and Atmos. Admin., Silver Spring, Md., 1987.

Lin, X., D. N. Baker, M. Temerin, T. Cayton, G. D. Reevs, T. Araki, H. Singer, D. Larson, R. P. Lin, and S. G. Kanekal, Energetic electron injections into the inner magnetosphere during the January 10–11, 1997, magnetic storm, *Geophys. Res. Lett.*, *25*, 2561–2564, 1998.

Moon, Y.-J., M. Dryer, Z. Smith, Y.-D. Park, and K.-S. Cho, A revised shock time of arrival (STOA) model for interplanetary shock propagation: STOA-2, *Geophys. Res. Lett.*, *29*(10), 1390, doi:10.1029/2002GL014865, 2002a.

Moon, Y.-J., G. S. Choe, H. Wang, Y.-D. Park, N. Gopalswamy, G. Yang, and S. Yashiro, A statistical study of two classes of coronal mass ejections, *Astrophys. J.*, *581*, 694–702, 2002b.

Neupert, W. M., B. J. Thompson, J. B. Gurman, and S. P. Plunkett, Eruption and acceleration of flare-associated coronal mass ejection loops in the low corona, *J. Geophys. Res.*, *160*, 25,215–25,226, 2001.

Oh, S. Y., Y. Yi, J.-S. Nah, and K.-S. Cho, Classification of the interplanetary shocks by shock drivers, *J. Korean Astron. Soc.*, *35*, 151–157, 2002.

Reiner, M. J., M. L. Kaiser, N. Gopalswamy, H. Aurass, G. Mann, A. Vourlidas, and M. Maksimovic, Statistical analysis of coronal shock dynamics implied by radio and white-light observations, *J. Geophys. Res.*, *106*, 25,279–25,290, 2001.

Shanmugaraju, A., Y.-J. Moon, M. Dryer, and S. Umapathy, An investigation of solar maximum metric type II radio bursts: Do two kinds of coronal shock sources exist?, *Solar Phys.*, *215*, 164–184, 2003.

Smart, D. F., and M. A. Shea, A simplified model for timing the arrival of solar flare-initiated shocks, *J. Geophys. Res.*, *90*, 183–190, 1985.

Smart, D. F., M. A. Shea, W. R. Barron, and M. Dryer, A simplified technique for estimating the arrival time of solar flare-initiated shocks, in *Proceedings of STIP Workshop on Solar/Interplanetary Intervals,*

August 4–6, 1982, Maynooth, Ireland, edited by M. A. Shea et al., pp. 139–156, BookCrafters, Chelsea, Mich., 1984.

Smith, Z., and M. Dryer, MHD study of temporal and spatial evolution of simulated interplanetary shocks in the ecliptic plane within 1 AU, *Solar Phys.*, *129*, 387–405, 1990.

Smith, Z., and M. Dryer, The Interplanetary Shock Propagation Model: A model for predicting solar-flare-caused geomagnetic sudden impulses based on the 2 1/2 D MHD numerical simulation results from the Interplanetary Global Model (2D IGM), *Tech. Memo. ERL/SEL-89*, Natl. Ocean. and Atmos. Admin., Silver Spring, Md., July 1995.

Smith, Z., M. Dryer, and M. Armstrong, Can soft X-rays be used as a proxy for total energy injected by a flare into the interplanetary medium?, in *Solar Coronal Structure*, *IAU Colloq.*, vol. 144, edited by V. Rusin, P. Heinsel, and J.-C. Vial, pp. 267–270, Kluwer Acad., Norwell, Mass., 1994.

Smith, Z., M. Dryer, E. Ort, and W. Murtagh, Performance of interplanetary shock prediction models: STOA and ISPM, *J. Atmos. Sol. Terr. Phys.*, *62*, 1265–1274, 2000.

Sun, W., M. Dryer, C. D. Fry, C. S. Deehr, Z. Smith, S.-I. Akasofu, M. D. Kartalev, and K. G. Grigorov, Real-time forecasting of ICME shock arrivals at L1 during the "April Fool's Day" Epoch: 28 March–21 April 2001, *Ann. Geophys.*, *20*, 937–945, 2002.

Svestka, Z., On "The Solar Flare Myth" postulated by Gosling, *Solar Phys.*, *160*, 53–56, 1995.

Thompson, B. J., J. B. Gurman, W. M. Neupert, J. S. Newmark, J.-P. Delaboudiniere, O. C. St. Cyr, S. Stezelberger, K. P. Dere, R. A. Howard, and D. J. Michels, SOHO/EIT observations of the 1997 April 7 coronal transient: Possible evidence of coronal moreton waves, *Astrophys. J.*, *517*, L151–L154, 2000.

Wagner, W. J., and R. M. McQueen, The excitation of type II radio bursts in the corona, *Astron. Astrophys.*, *120*, 136–138, 1983.

Wu, S. T., H. Zheng, S. Wang, B. J. Thompson, S. P. Plunkett, X. P. Zhao, and M. Dryer, Three-dimensional numerical simulation of MHD waves observed by the Extreme Ultraviolet Imaging Telescope, *J. Geophys. Res.*, *106*, 25,089–25,102, 2001.

Zhang, J., K. P. Dere, R. A. Howard, M. R. Kundu, and S. M. White, On the temporal relationship between coronal mass ejections and flares, *Astrophys. J.*, *559*, 452–462, 2001.

K.-S. Cho, Y.-J. Moon, and Y.-D. Park, Korea Astronomy Observatory, Daejon, Republic of Korea. (kscho@kao.re.kr; yjmoon@kao.re.kr; ydpark@ kao.re.kr)

M. Dryer, Space Environment Center, National Oceanic and Atmospheric Administration, Boulder, CO 80303-3328, USA. (murray.dryer@noaa.gov)

C. D. Fry, Exploration Physics International, Inc., Suite 37-105, 6275 University Drive, Huntsville, AL 35806-1776, USA. (gfry@expi.com)

K.-S. Kim, Department of Astronomy and Space Science, Kyung Hee University, Kyunggi-do 449-771, Korea. (kskim@khu.ac.kr)